Relating solvent parameters to electrochemical properties to predict the electrochemical performance of Vanadium acetylacetonate for non-aqueous redox flow batteries

Thomas Stracensky[1,2], Rangachary Mukundan[2, 3], Sandip Maurya*[,2], Sanjeev Mukerjee*[,1]

[1]Department of Chemistry and Chemical Biology, Northeastern University, Boston, Massachusetts, 02115, United States

[2] Materials Physics and Applications Division, Los Alamos National Laboratory, Los Alamos, NM 87545, United States

3 Energy Technology area, Lawrence Berkeley National Laboratory, 1 Cyclotron Road

Berkeley, CA 94720, United States

*Correspondence author email: s.mukerjee@northeastern.edu; smaurya@lanl.gov

Abstract

Non-aqueous redox flow batteries have shown promise for applications in grid energy storage. [why this investigation is needed] Herein, we investigate the correlation between solvent properties and the electrochemical parameters of vanadium acetylacetonate $V(acac)_3$. Using cyclic voltammetry (CV) and rotating disk electrode experiments (RDE), we show that trends in the performance of the $V(acac)_3$ kinetics are directly related to solvent properties. [some highlight of your work]. Based on these finding, we also demonstrate how solvent selection can be improved with limited a priori knowledge.

1. Introduction

Due to inconsistencies with power demand and power generation from renewable resources such as wind and solar, energy needs to be supplied during peak demand and stored during times of high-power generation.[1–3] Redox flow batteries (RFBs) have promise in the field of grid energy storage to address the demand shift application.[4] Redox flow batteries are uniquely constructed to decouple the power and energy through the separation of the electrolyte storage tanks and the electrode to allow for very tunable applications.[5] Creating a cost-effective system by increasing energy density is a major drive in the field of RFBs.[6] One method to increase energy density is through the use of non-aqueous electrolytes, which are not subject to oxygen evolution and hydrogen evolution reactions that limit the stability window of aqueous systems. Some electrolytes provide voltage windows >4 V allowing for the possibility of high energy density storage. Currently, several groups have looked to take advantage of the non-aqueous RFB's large voltage window by design and selection of redox couples with large potential differences with the goal of increasing the energy density.[7–12]

The gold standard of non-aqueous redox flow batteries is the vanadium acetylacetonate ($V(acac)_3$) system. This system forms a symmetric RFB with $V(acac)_3$ acting as both the

catholyte and anolyte for the RFB. The multiple redox states available to vanadium allow for a V(II/III) couple on the negative side and a V(III/IV) couple on the positive side and can achieve a voltage of ~2.2 V.[13] The major benefit of the symmetric RFB is the mitigation of capacity loss caused by the crossover of the active species.[14] Specifically for $V(acac)_3$, this complex has stable redox events positioned on the vanadium center, which resolves issues associated with non-innocent ligands in redox flow batteries which can lead to instability of the radical ion located on the ligand.[15]

An important focus of RFBs in general and for the $V(acac)_3$ system specifically is understanding the effects of solvents and supporting electrolytes on the thermodynamic and kinetic properties of the system. The focus of this research for the $V(acac)_3$ system done by Herr et al. has been on the solvent and supporting electrolyte effect on solubility and conductivity of the electrolyte.[16] Mixed solvent systems with binary or ternary compositions have also been investigated and are an attractive approach to optimize solvent properties with continued interest in the solubility and conductivities of the mixtures towards increasing the energy density of the system.[17] Work by Bamgbopa et al. further increased upon this work through a systematic investigation of solvent mixtures' thermodynamic properties such as density, molar volume, viscosity, solubility, and diffusion, as well as electrochemical properties such as the heterogeneous rate constant for the electron transfer reaction.[18]

While previous work has investigated the effects of solvent on solution resistance and solubility, little work has been done to investigate what fundamental properties of an electrolyte make it suitable for a nonaqueous redox flow battery. Predominately solvents are selected by a trial-and-error approach where the properties that make a solvent desirable are mostly unknown. Herein we look at the vanadium acetylacetonate system to investigate the solvent effects on electrochemical kinetics and thermodynamic parameters of the system with cyclic voltammetry

and rotating disk electrode techniques and identify the influence of electrolyte properties on these parameters. We also investigate the effect of donor number on the stability of the $V(acac)_3$ system towards high potential cycling and will discuss it herein.

2. Experimental and materials

Electrolytes

Electrolyte solutions were prepared by dissolving $V(acac)_3$ (98%, STREM) at 5 mM and tetraethylammonium tetrafluoroborate (TEA-BF_4) (99%, Sigma Aldrich) at 500 mM into a solvent of either: acetonitrile (ACN) (99.8%, anhydrous, Sigma Aldrich), propylene carbonate (PC) (99.7%, anhydrous, Sigma Aldrich), dimethyl sulfoxide (DMSO) (99.8%, anhydrous, Alfa Aesar), N,N-dimethylformamide (DMF) (99.8%, anhydrous, Sigma Aldrich), N-methylformamide (NMF) (99%, Sigma Aldrich) or dimethylacetamide (DMAc) (99.8%, anhydrous, Sigma Aldrich). All materials were stored and prepared in a glove box under inert argon gas (<0.1ppm O_2, <0.1ppm H_2O). The kinematic viscosities of each electrolyte were determined using a Cannon-Fenske size 25 or size 75 viscometer at 22±1 °C.

Cyclic voltammetry experiments

All electrochemistry experiments were performed in a glove box under inert argon gas. Cyclic voltammetry was performed using an SP-150 potentiostat (Biologic) and a traditional three-electrode system using a BluRev rotating ring disk electrode (RRDE) fitted with a 0.196 cm^2 glassy carbon working electrode, a Basi Ag/Ag^+ electrode that was prepared with 10 mM $AgNO_3$ (Sigma Aldrich) in 100 mM TEA-BF_4/acetonitrile was used as a reference, and a graphite rod was used as a counter electrode. The potential range were scanned at various scan rates of 10, 20,

50, 75, 100, 200, 300, and 500 mV/s. In the RDE experiments, the rotation rates of the working electrode were 300, 600, 900, 1200, 1600, and 2500 RPM.

The diffusion coefficients were calculated from the CVs using the Randles-Sevick equation for a reversible electron transfer,

$$i_p = 2.69 \times 10^5 n^{\frac{3}{2}} A D^{\frac{1}{2}} C \nu^{\frac{1}{2}} \quad \text{(Eq. 1)}$$

Where the i_p is the peak current (A), n is the number of electrons transferred, A is the geometrical surface area (cm^2), D is the diffusion coefficient ($cm^2\ s^{-1}$) of the relevant species, C is the concentration of the redox species (mol cm^{-3}), and ν is the scan rate ($V\ s^{-1}$). The diffusion coefficient was determined from the Randles-Sevick plot of the slope of the i_p versus $\nu^{1/2}$ plot. Peak currents were obtained from linear baseline correction of the CVs.

The RDE experiments utilize solution convection leading to limiting currents (Levich currents) at high overpotentials. The diffusion coefficient of the neutral species can then also be determined from the Levich equation,

$$I_L = (0.620) n F A D^{\frac{2}{3}} \upsilon^{\frac{-1}{6}} C \omega^{\frac{1}{2}} \quad \text{(Eq. 2)}$$

Where I_L is the Levich current, F is Faraday constant (C mol^{-1}), υ is the kinematic viscosity ($cm^2\ s^{-1}$) measured using Cannon-Fenske viscometer, and ω is the rotation rate of the working electrode (rad s^{-1}).

The kinetic current was determined for five different overpotentials potentials in the mixed transport/kinetic limited current region of the RDE curves at 2500, 1600, 1200, and 900 RPM by the Koutecky-Levich equation,

$$\frac{1}{i_m} = \frac{1}{i_k} + \frac{1}{0.620 n F A D^{\frac{2}{3}} \omega^{\frac{1}{2}} \upsilon^{\frac{-1}{6}} C} \quad \text{(Eq. 3)}$$

Where i_m is the measured current and i_k is the kinetic current.

The kinetic parameters of the electron transfer were then determined by the Tafel equation using the kinetic currents obtained from the Koutecky-Levich plot.

$$logi_k = Logi_0 + \frac{(1-\alpha)nF\eta}{2.3RT} \quad \text{(Eq. 4)}$$

Where i_0 is the exchange current density (A cm^{-2}), α is the charge transfer coefficient, R is the universal gas constant (J mol^{-1} K^{-1}), and η is the reaction overpotential (V). The heterogeneous rate constant can then be determined from the exchange current density by the Butler-Volmer equation

$$i_0 = nFCk_0 \quad \text{(Eq. 5)}$$

Where k_0 is the heterogeneous reaction rate constant (cm s^{-1}).

The Stokes-Einstein relationship describes the situation where the diffusion coefficient (D) is proportional to Boltzmann's constant (κ) and temperature (T) and inversely proportional to the hydrodynamic radius (α) and the viscosity of the solution (η).

$$D = \frac{\kappa T}{6\pi\eta\alpha} \quad \text{(Eq. 6)}$$

3. Results and discussions

In non-aqueous electrolytes, vanadium acetylacetonate demonstrates two one-electron redox events:

$[V(acac)3]^0 + e^- \leftrightarrow [V(acac)3]^-$ (Eq. 7)

$[V(acac)3]^+ + e^- \leftrightarrow [V(acac)3]^0$ (Eq. 8)

Both are associated with an electron transfer on the central vanadium atom of the complex, changing the oxidation state (II/III) at the negative potentials (**Equation 7**) and (III/IV) at more positive potentials (**Equation 8**). The effects of solvents on the $V(acac)_3$ were investigated by

cyclic voltammetry (CV) experiments (**Figure 1A-F**). All solvents show a slight increase in peak separation for both the V (II/III) and V(III/IV) redox couples as the sweep rate was increased from 5 mV/s to 500 mV/s signifying the $V(acac)_3$ transitions are quasi reversible in all the solvents tested. Four solvents, DMF, DMSO, DMAc, and NMF showed a feature past the vanadium (III/IV) redox peak that is often associated with the formation of vanadyl acetylacetonate.[19] This noticeably affects the vanadium (III/IV) redox couple, where the reduction peak shrinks with lower scan rates and an increased number of scans. Additionally, when the potential is scanned to the negative region, the evolution of a redox peak at -1.5 V vs. Ag/Ag^+ is observed which is associated with the degradation occurring at higher negative potentials.

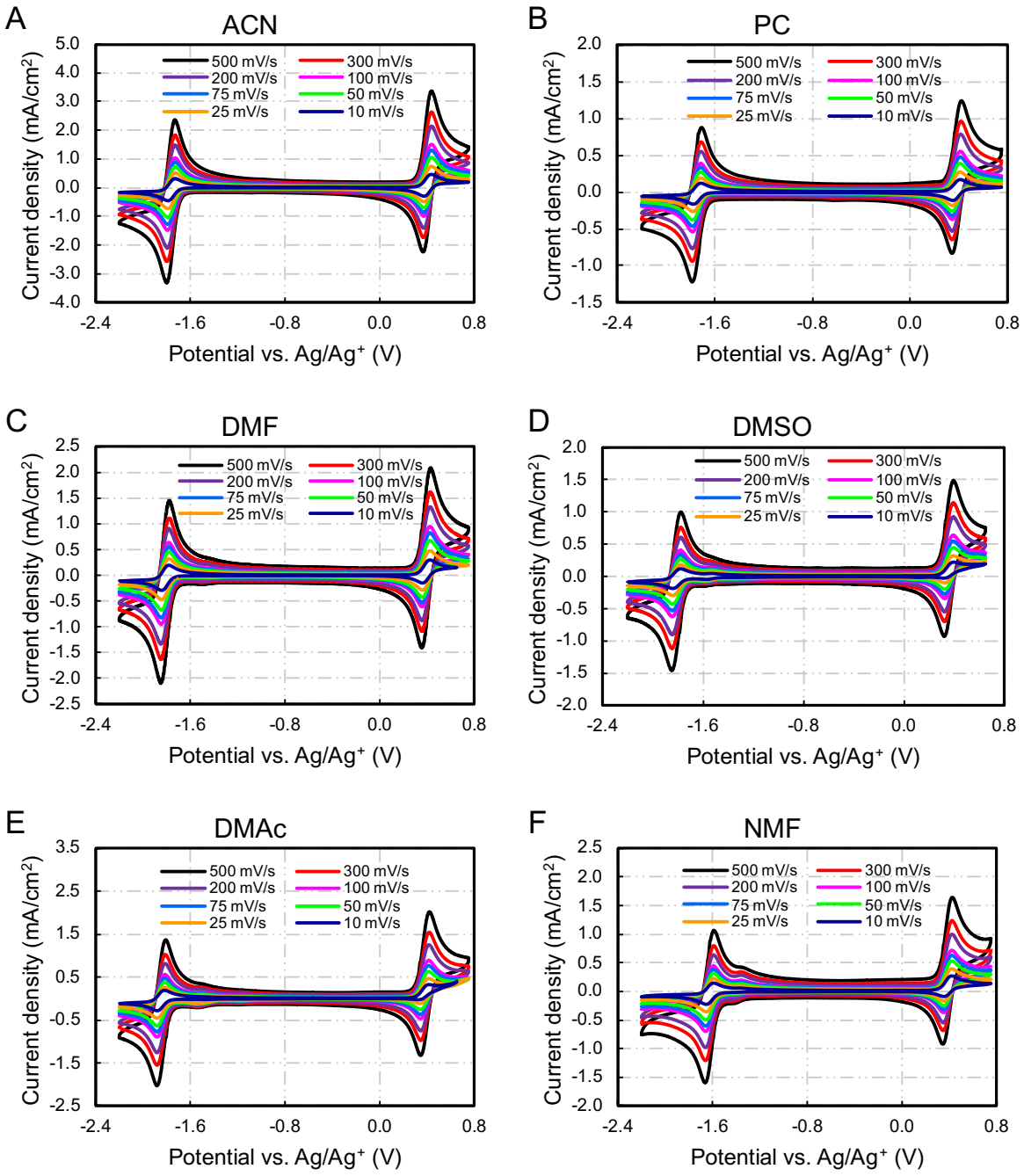

Figure 1: Cyclic voltammetry of 5mM $V(acac)_3$ 10th scan at scan rates ranging from 10-500 mV/s in various solvents; acetonitrile (A), dimethyl sulfoxide (B), propylene carbonate (C), N,N-dimethylformamide (D), N,N-dimethylacetamide (E) and N-methylformamide (F).

From the CVs, the position of the peak potentials is seen to be dependent on the solvent for both the V(II/III) and V(III/IV) redox events. The CV data was also analyzed using the

Randles-Sevcik relationship to determine the diffusion coefficients of the species (**Equation 1**). The Randles-Sevcik derived plots showed strongly linear relationships of I_p with the square root of scan rate (ν) for both the V (II/III) redox couple and for the V(III/IV) couple (**Figure S1**) indicating a diffusion-controlled reaction without adsorption of the redox active $V(acac)_3$ onto the electrode and covered nearly an order of magnitude difference for the various solvents. The change in the diffusion coefficient of the neutral species when analyzing both the positive V(III/IV) couple and the negative V(II/III) couple showed good agreement with each other, indicating the system was well-behaved. The electrochemical parameters obtained via CV measurements were compiled in **Table 1**.

Table 1: Electrochemical parameters of $V(acac)_3$ in various solvents

Solvent	Redox	E^0 (V) vs. Ag/Ag^+	D_0 ($cm^2\ s^{-1}$)	D_+ ($cm^2\ s^{-1}$)	D_- ($cm^2\ s^{-1}$)	k^0 ($cm\ s^{-1}$)
ACN	(III/IV)	0.404	$1.11x10^{-5}$	$9.04x10^{-6}$		-
	(II/III)	-1.762	$1.10x10^{-5}$		$9.44x10^{-6}$	0.042
PC	(III/IV)	0.381	$1.24x10^{-6}$	$1.15x10^{-6}$		-
	(II/III)	-1.751	$1.34x10^{-6}$		$1.21x10^{-6}$	0.0096
DMF	(III/IV)	0.392	$3.98x10^{-6}$	$3.43x10^{-6}$		-
	(II/III)	-1.815	$4.01x10^{-6}$		$3.46x10^{-6}$	0.022
DMSO	(III/IV)	0.363	$1.74x10^{-6}$	$2.09x10^{-6}$		-
	(II/III)	-1.812	$1.90x10^{-6}$		$2.00x10^{-6}$	0.010
DMAc	(III/IV)	0.381	$3.77x10^{-6}$	$3.73x10^{-6}$		-
	(II/III)	-1.849	$3.77x10^{-6}$		$3.22x10^{-6}$	0.024
NMF	(III/IV)	0.386	$1.99x10^{-6}$	$1.62x10^{-6}$		-
	(II/III)	-1.625	$1.98x10^{-6}$		$1.77x10^{-6}$	0.011

Rotating disk electrode (RDE) experiments were also conducted with a 10 mV/s scan rate at various disk rotation rates (**Figure S2**). Here the diffusion coefficient was calculated for the

neutral species using the Levich relationship shown in **Equation 2** from plots of the Levich current vs. the square root of the rotation rate (**Figure S3**). These values matched well with those obtained via the CV technique but were generally higher. This may be caused by the fact the Randles-Sevcik equations assume a perfectly kinetically reversible system which is not necessarily the case in all solvents. Five potentials in the mixed kinetic and mass transport regions of the LSV curves were selected and analyzed Koutecky-Levich equation (**Equation 3**) to determine the kinetic currents of the $V(acac)_3$ in each of the solvents. The kinetic currents were then used in the Tafel equation (**Equation 4**) to determine the heterogenous rate constants (k^0) of the V(II/III) electron transfer event in the various solvents and added to **Table 1**.

While it is important to investigate the properties of the redox active species in the various solvents, the parameter of the solvent that affects the chemical and electrochemical properties is paramount for understanding solvent system design. **Table 2** shows different parameters of the pure solvent unless otherwise noted, that were identified as influential towards the chemical/electrochemical behavior of $V(acac)_3$. Donor number was identified as a key factor in determining the stability of the V(III/IV) redox couple to extended cycling at positive potentials. High donor solvents such as DMSO, DMF, DMAc, and NMF are seen to undergo a unique degradation pathway not seen in the low donor number solvents, ACN, and PC, as discussed previously. When cycling at positive potentials, >0 V vs. Ag/Ag^+, the evolution of a second redox peak is seen, while a concurrent decrease of the first redox peak is also observed (**Figure 2A**). In literature, the degradation mechanism of the $V(acac)_3$ complex is often attributed to the formation of vanadyl acetylacetonate which, is attributed to the second positive redox couple.[13,17,19,24]

Table 4.1: Solvent parameters

Parameter	ACN	DMSO	PC	DMF	DMAc	NMF
Permittivity constant[20]	35.9	46.5	64.9	36.7	37.9	182.4
Viscosity* (cP)	0.48	2.5	3.1	1.22	1.38	2.00
Donor # (kcal mol^{-1})[21,22]	14.1	29.8	15.1	26.6	27.8	27
Acceptor # (kcal mol^{-1})[21,22]	18.9	19.3	18.3	16.0	13.6	32.1
Normalized Dimroth-Reichardt parameter[20]	0.460	0.444	0.472	0.386	0.377	0.722
Longitudinal relaxation time (ps)[23]	0.2	2.4	2.7	1.3	1.5	3.7

*Viscosity of solvent containing 0.5 M TEA-BF4 and 0.005 M $V(acac)_3$

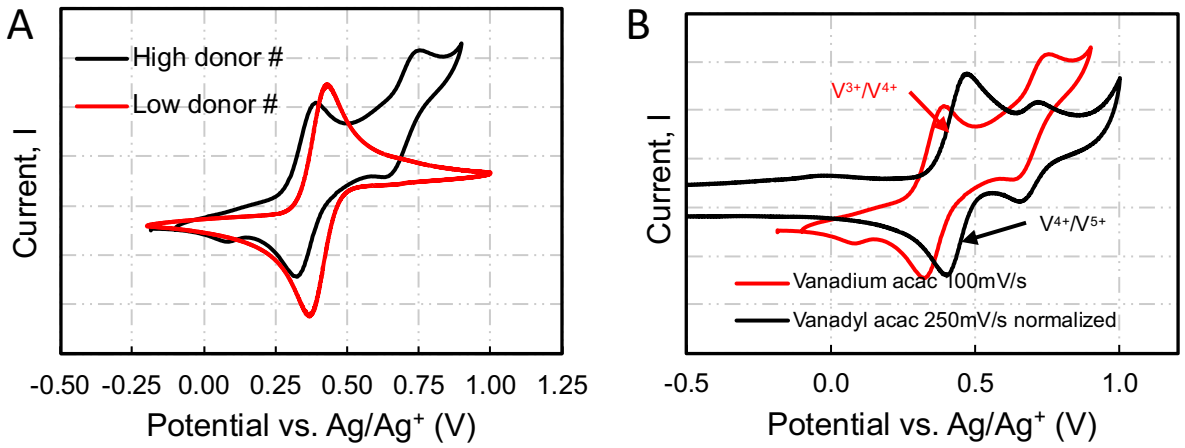

Figure 2: Cyclic voltammetry of $V(acac)_3$ in high donor number solvent (DMSO) and low donor number solvent (ACN) (A). Labeled peaks of vanadium acetylacetonate and vanadyl acetylacetonate in DMSO (B).

We investigated the vanadyl acetylacetonate in DMSO, which showed a quasi-reversible redox peak at ~0.47 V vs. Ag/Ag^+ and, upon extended cycling, a second peak at ~0.7 V vs. Ag/Ag^+ **Figure 3B**). When compared to the $V(acac)_3$ peaks, it did not match the V (III/IV) transition peak at 0.36 V Ag/Ag^+, or the evolved peak at 0.7 V vs. Ag/Ag^+, indicating that this evolved peak was indeed not indicative of the formation of vanadyl acetylacetonate. When vanadyl acetylacetonate was cycled at positive potentials over time in DMSO, the evolution of the peak at 0.7 V vs. Ag/Ag^+ was again observed, and it appeared to evolve even quicker than was seen for the $V(acac)_3$. This 0.7 V peak is not to be considered a V(V/VI) transition as $V(acac)_3$ has the same peak but does not undergo a (IV/V) transition. It seems this second peak is not immediately accessible on the first scan for either $V(acac)_3$ or the vanadyl acetylacetonate complex but is evolved after high potential cycling, indicating a chemical reaction on the positively charged state occurs after the complex is oxidized, suggesting an electrochemical-chemical mechanism, where both oxidized complexes, vanadyl acetylacetonate and $V(acac)_3$, are forming the same product. Previous work into the effects of high donor number solvents on electrochemical reaction products has been done by Laoire et al. and demonstrated that high donor solvent could stabilize the $Li\text{-}O_2^-$ adduct.[25] This was explained by hard soft acid base theory, where the high donor number solvent was able to solvate the hard lithium acid. He Qi et al. also observed this for S-Li batteries where in the presence of hard Li counter ions, a high donor number solvent could drive the reaction toward the formation of softer anion products.[26] In this work, we believe the higher donor number solvent, such as seen with DMSO, is directly coordinating with the cationic degradation product, which stabilizes this product.

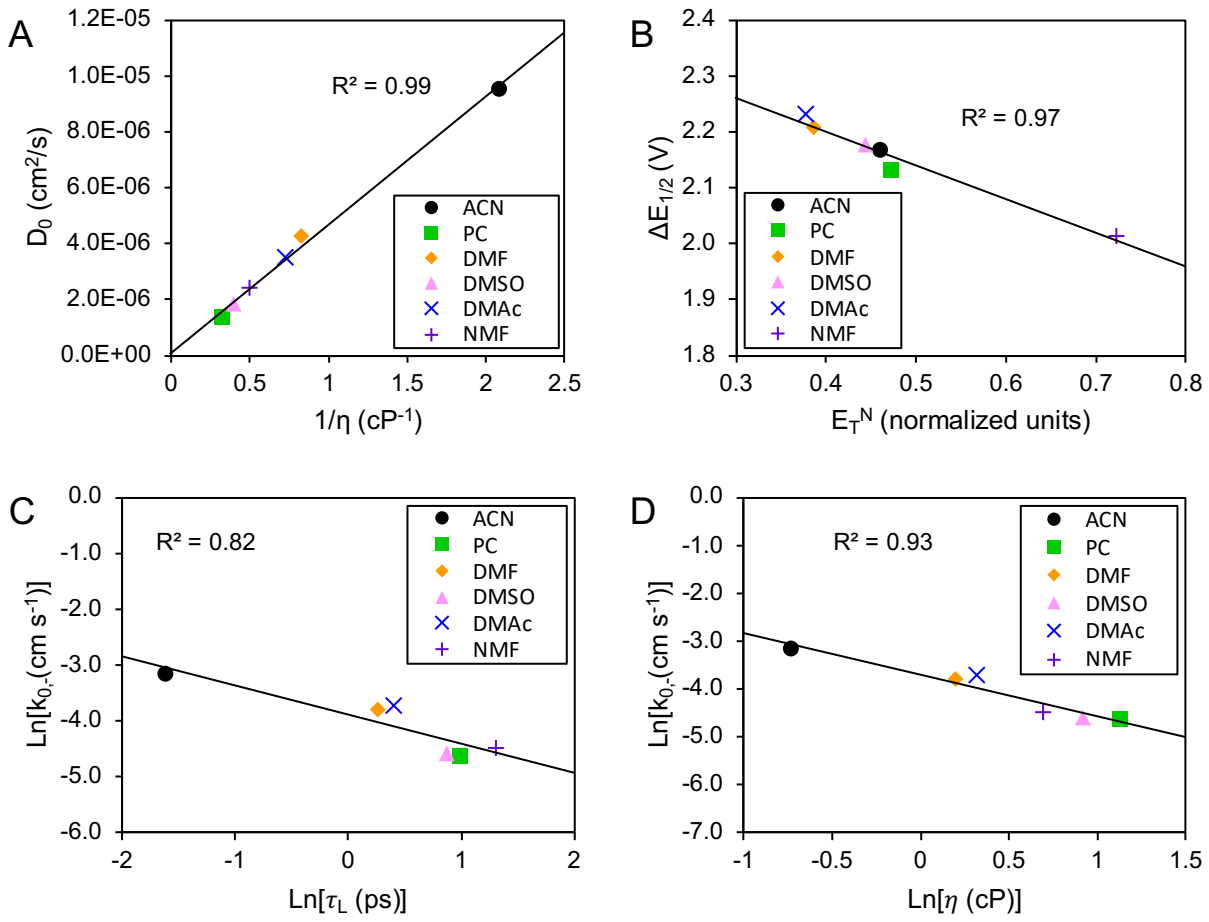

Figure 3: Correlation plots of solvent properties with measured electrochemical parameters. Relationship between the diffusion coefficient and the obtained from Levich analysis and the inverse of the viscosity of the electrolyte (A). Relationship of the difference between the redox potential of the V(II/III) and V(III/IV) couple and the normalized Dimroth-Reichardt parameter (B). Double natural logarithm correlation between the rate constant of vanadium and the longitudinal relaxation time of the solvent (C). Double natural logarithm correlation plot of the rate constant of vanadium and the viscosity of the electrolyte (D).

Further investigation of other solvent parameters on the behavior of $V(acac)_3$ yielded several trends. The first trend was the relationship between the diffusion coefficient of the neutral species to the reciprocal of the solvent viscosity (**Figure 3A**). This can be explained by the Stokes-Einstein relationship (**Equation 6**), where the diffusion coefficient is inversely proportional to solvent viscosity if the hydrodynamic radius does not change. The strong linear correlation between the diffusion coefficient and the reciprocal of viscosity demonstrates there

was little change in the hydrodynamic radius of vanadium acetylacetonate (III) species in the solvents selected. The average hydrodynamic radius was calculated from the slope of the curve and found to be 0.48 nm which has not been reported to this point. This value is slightly larger than that of the vanadyl acetylacetonate was determined to be 0.38 nm by Hwang et al.[27] This is expected as vanadyl acetylacetonate has one acetylacetonate ligand replaced with a single oxygen atom and would expectedly be smaller. This allows for control of the diffusion coefficient of the redox species by the viscosity of the electrolyte used.

In an all-vanadium acetylacetonate battery, the gap between the standard potential of V (II/III) and the V(III/IV) redox couples determines the theoretical open circuit voltage of the battery and thus can influence the energy density that can be achieved. This gap was seen to be dependent on the solvent used, where it varied between 2.231 V in DMAc and 2.011 V in NMF. When this voltage difference was paired with the normalized Dimroth-Reichardt parameter (E_T^N), a high-fidelity linear trend emerged, even when the highly polar and protic solvent NMF was used (**Figure 3B**). The E_T^N is an empirical measure of a solvent's polarity, determined by the ability of a solvent to stabilize the transition state of N-phenolate betaine dye as seen by UV-Vis spectra.[28] This can be understood by the formation of charged complexes. As previously shown, $V(acac)_3$ forms a cationic complex upon oxidation at the positive electrode (**Equation 7**) and an anionic complex upon reduction at the negative electrode to the anionic complex (**Equation 8**). The increased ability to solvate these charged species by polar solvents results in a lower potential difference between the two redox potentials. In this case, it is seen the stabilization of the negatively charged anionic vanadium complex by the polar solvent is the more important of the two charge complexes. This is noticed by the variance of the redox potentials for the V(II/III) couple is greater than 200 mV in the various solvents, while the V(III/IV) couple varies by only 35 mV. While the solvent effect on changes in potential has been

reported before for transition metal complexes, it is often reported versus the Fc couple, which itself changes between solvents but not the separation of potentials of various redox states on the same complex. Here a single descriptor of solvent polarity was adequate to describe the expected change in the peak separation in various solvents.

The kinetics of $V(acac)_3^0$ reduction was investigated in the six solvents by RDE experiments at various rotation rates. Koutecky-Levich analysis of the RDE plots was done to determine kinetic currents at various potentials, which were used to construct Tafel plots to determine the rate electron transfer process. This study shows there is a linear relationship between the natural logarithm of the rate constant (**Figure 3C**) of the electron transfer of the reduction of V(III->II) (k^0) and the natural logarithm of the longitudinal relaxation time (τ_L), with shorter relaxation times realizing faster electron transfer kinetics. This observation between the rate constant and the solvent's longitudinal relaxation time has been observed in several systems in the literature.[29–34] This relationship can be explained on the bases of Marcus theory for an electron transfer. Marcus theory has been used as the basis for understanding electron transfer reactions and is governed by the following equation.

$$k^0 = A\tau_L^{-\theta} e^{\left(-\frac{\Delta G^{\ddagger}_{o/s} + \Delta G^{\ddagger}_{i/s}}{RT}\right)} \qquad \text{(Eq. 4.9)}$$

Where A is the preexponential factor, haa some solvent-specific dependence but can be considered minimal and neglected in some common cases[35], θ is a measure of reactions' adiabaticity ranging from 0 to 1, $\Delta G^{\ddagger}_{o/s}$ is the outer sphere change in the Gibbs free energy of activation, and $\Delta G^{\ddagger}_{i/s}$ is the inner sphere change in the Gibbs free energy of activation. When the major contribution to the kinetics is from the longitudinal relaxation time, a linear trend between the natural logarithm of k^0 and the natural logarithm of τ_L with a slope of $-\theta$. For the solvents tested, the $V(acac)_3$ system obeyed this trend, even with the protic NMF solvent. The natural

logarithm of the electrolyte viscosity also showed a linear correlation with the electron transfer rate, as has been demonstrated by other researchers.[31,36,37] In our $V(acac)_3$ system, we obtained a linear correlation of even higher fidelity than the longitudinal relaxation time (**Figure 3D**). Here low viscosity electrolytes, such as the ACN electrolyte, were seen to give an increased k^0 over the more viscous electrolyte, such as PC.

These correlations can be translated into an understanding of methods to address overpotentials in flow batteries by solvent system design. The major source of overpotentials can be described broadly by three current ranges in **Figure 4**. The first is at a low current density where overpotential from the kinetics of the electron transfer process is dominant. This can be addressed through the solution permittivity constant that was shown to affect the rate constant of the electron transfer. The second area is where the resistance is the main source of overpotential. This can be addressed by looking at the solubility of the salts in the electrolyte and by developing membranes with lower resistance for ionic transport of the supporting electrolyte. The last region is the mass transport region which can be reduced physically via increased pump rate and by lowering the viscosity of the solution, which has the dual effect of lowering the energy requirements of the pump while also increasing the diffusion coefficient, which allows for lower overpotentials at high currents.

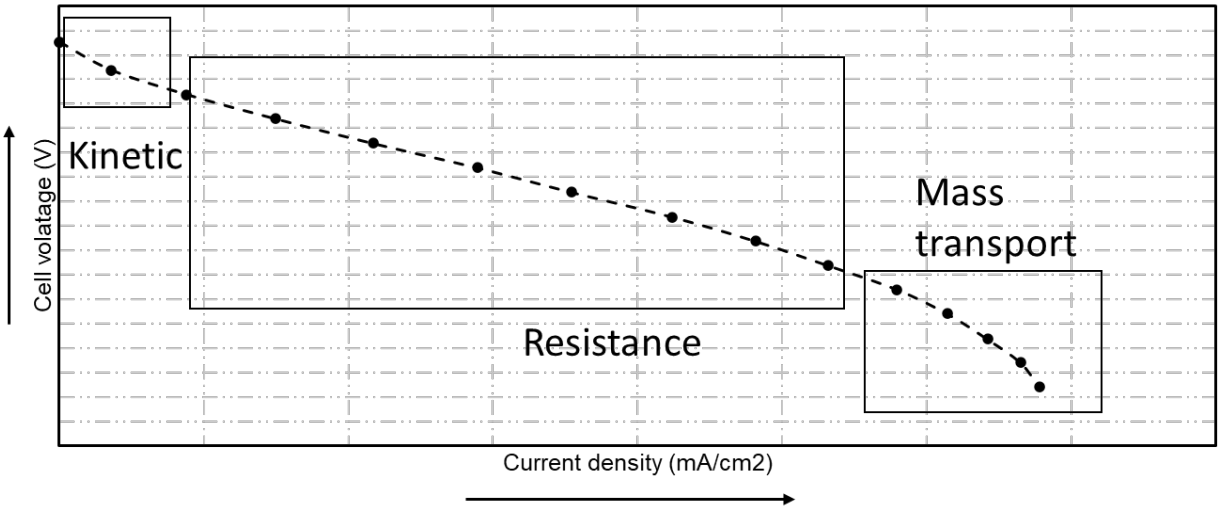

Figure 4: Demonstration of sources of overpotential for a redox flow battery at various current densities.

4. Conclusions

In this work we observed how solvents changed the electrochemical parameters of the electron transfer process. We then looked at key solvent parameters and showed how they affect each parameter for V(acac) complex. We propose this in-depth analysis of solvent effects on the electrochemical properties of the $V(acac)_3$ system can be extended to other systems and give a principle-based design methodology for examining solvent and supporting electrolyte, providing an alternative from the trial-and-error approach oft employed is solvent selection for non-aqueous redox flow batteries.

5. Acknowledgments

Financial support from the Office of Electricity, US department of Energy and Dr. Imre Gyuk (Director, Energy Storage Research. US Department of Energy)

6. References

(1) Wedege, K.; Azevedo, J.; Khataee, A.; Bentien, A.; Mendes, A. Direct Solar Charging of an Organic–Inorganic, Stable, and Aqueous Alkaline Redox Flow Battery with a Hematite Photoanode. *Angew. Chemie Int. Ed.* **2016**, *55* (25), 7142–7147.
(2) Ma, S.; Xu, Y. P.; Li, X. F.; Wang, Y. F.; Zhang, N.; Xu, Y. R.; Ma, S.; Xu, Y. P.; Li, X. F.; Wang, Y. F.; et al. Research on Reduction of Solar Power Curtailment with Grid Connected Energy Storage System Based on Time-Series Production Simulation. *Energy Power Eng.* **2017**, *9* (4), 162–175.
(3) Ponce de León, C.; Frías-Ferrer, A.; González-García, J.; Szánto, D. A.; Walsh, F. C. Redox Flow Cells for Energy Conversion. *J. Power Sources* **2006**, *160* (1), 716–732.
(4) Sánchez-Díez, E.; Ventosa, E.; Guarnieri, M.; Trovò, A.; Flox, C.; Marcilla, R.; Soavi, F.; Mazur, P.; Aranzabe, E.; Ferret, R. Redox Flow Batteries: Status and Perspective towards Sustainable Stationary Energy Storage. *J. Power Sources* **2021**, *481*, 228804.
(5) Yang, Z.; Zhang, J.; Kintner-Meyer, M. C. W.; Lu, X.; Choi, D.; Lemmon, J. P.; Liu, J. Electrochemical Energy Storage for Green Grid. *Chem. Rev.* **2011**, *111* (5), 3577–3613.
(6) Tang, L.; Leung, P.; Xu, Q.; Mohamed, M. R.; Dai, S.; Zhu, X.; Flox, C.; Shah, A. A. Future Perspective on Redox Flow Batteries: Aqueous versus Nonaqueous Electrolytes. *Curr. Opin. Chem. Eng.* **2022**, *37*, 100833.
(7) Pahlevaninezhad, M.; Leung, P.; Velasco, P. Q.; Pahlevani, M.; Walsh, F. C.; Roberts, E. P. L.; Ponce De León, C. A Nonaqueous Organic Redox Flow Battery Using Multi-Electron Quinone Molecules. *J. Power Sources* **2021**, *500*, 229942.
(8) Cammack, C. X.; Pratt, H. D.; Small, L. J.; Anderson, T. M. A Higher Voltage Fe(II) Bipyridine Complex for Non-Aqueous Redox Flow Batteries. *Dalt. Trans.* **2021**, *50* (3), 858–868.
(9) Wei, X.; Xu, W.; Huang, J.; Zhang, L.; Walter, E.; Lawrence, C.; Vijayakumar, M.; Henderson, W. A.; Liu, T.; Cosimbescu, L.; et al. Radical Compatibility with Nonaqueous Electrolytes and Its Impact on an All-Organic Redox Flow Battery. *Angew. Chemie* **2015**, *127* (30), 8808–8811.
(10) Oh, S. H.; Lee, C. W.; Chun, D. H.; Jeon, J. D.; Shim, J.; Shin, K. H.; Yang, J. H. A Metal-Free and All-Organic Redox Flow Battery with Polythiophene as the Electroactive Species. *J. Mater. Chem. A* **2014**, *2* (47), 19994–19998.
(11) Yan, Y.; Robinson, S. G.; Sigman, M. S.; Sanford, M. S. Mechanism-Based Design of a High-Potential Catholyte Enables a 3.2 v All-Organic Nonaqueous Redox Flow Battery. *J. Am. Chem. Soc.* **2019**, *141* (38), 15301–15306.
(12) Xing, X.; Huo, Y.; Wang, X.; Zhao, Y.; Li, Y. A Benzophenone-Based Anolyte for High Energy Density All-Organic Redox Flow Battery. *Int. J. Hydrogen Energy* **2017**, *42* (27), 17488–17494.
(13) Liu, Q.; Sleightholme, A. E. S.; Shinkle, A. A.; Li, Y.; Thompson, L. T. Non-Aqueous Vanadium Acetylacetonate Electrolyte for Redox Flow Batteries. *Electrochem. commun.* **2009**, *11* (12), 2312–2315.
(14) Rhodes, Z.; Cabrera-Pardo, J. R.; Li, M.; Minteer, S. D. Electrochemical Advances in Non-Aqueous Redox Flow Batteries. *Isr. J. Chem.* **2021**, *61* (1–2), 101–112.
(15) Li, B.; Liu, J. Progress and Directions in Low-Cost Redox-Flow Batteries for Large-Scale Energy Storage. *Natl. Sci. Rev.* **2017**, *4* (1), 91–105.
(16) Herr, T.; Noack, J.; Fischer, P.; Tübke, J. 1,3-Dioxolane, Tetrahydrofuran, Acetylacetone and Dimethyl Sulfoxide as Solvents for Non-Aqueous Vanadium Acetylacetonate Redox-Flow-Batteries. *Electrochim. Acta* **2013**, *113*, 127–133.
(17) Herr, T.; Fischer, P.; Tübke, J.; Pinkwart, K.; Elsner, P. Increasing the Energy Density of the Non-Aqueous Vanadium Redox Flow Battery with the Acetonitrile-1,3-Dioxolane-

Dimethyl Sulfoxide Solvent Mixture. *J. Power Sources* **2014**, *265*, 317–324.
(18) Bamgbopa, M. O.; Pour, N.; Shao-Horn, Y.; Almheiri, S. Systematic Selection of Solvent Mixtures for Non-Aqueous Redox Flow Batteries – Vanadium Acetylacetonate as a Model System. *Electrochim. Acta* **2017**, *223*, 115–123.
(19) Shinkle, A. A.; Sleightholme, A. E. S.; Griffith, L. D.; Thompson, L. T.; Monroe, C. W. Degradation Mechanisms in the Non-Aqueous Vanadium Acetylacetonate Redox Flow Battery. *J. Power Sources* **2012**, *206*, 490–496.
(20) Reichardt, C.; Welton, T. Appendix A. Properties, Purification, and Use of Organic Solvents. In *Solvents and Solvent Effects in Organic Chemistry*; 2010; pp 549–586.
(21) Izutsu, K. Properties of Solvents and Solvent Classification. In *Electrochemistry in Nonaqueous Solutions*; 2002; pp 1–24.
(22) Gritzner, G. Solvent Effects on Redox Potentials: Studies in N-Methylformamide. *J. Electroanal. Chem. Interfacial Electrochem.* **1983**, *144* (1–2), 259–277.
(23) McManis, G. E.; Neal Golovin, M.; Weaver, M. J. Role of Solvent Reorganization Dynamics in Electron-Transfer Processes. Anomalous Kinetic Behavior in Alcohol Solvents. *J. Phys. Chem.* **1986**, *90* (24), 6563–6570.
(24) Herr, T.; Noack, J.; Fischer, P.; Tübke, J. 1,3-Dioxolane, Tetrahydrofuran, Acetylacetone and Dimethyl Sulfoxide as Solvents for Non-Aqueous Vanadium Acetylacetonate Redox-Flow-Batteries. *Electrochim. Acta* **2013**, *113*, 127–133.
(25) Laoire, C. O.; Mukerjee, S.; Abraham, K. M.; Plichta, E. J.; Hendrickson, M. A. Influence of Nonaqueous Solvents on the Electrochemistry of Oxygen in the Rechargeable Lithium-Air Battery. *J. Phys. Chem. C* **2010**, *114* (19), 9178–9186.
(26) He, Q.; Gorlin, Y.; Patel, M. U. M.; Gasteiger, H. A.; Lu, Y.-C. Unraveling the Correlation between Solvent Properties and Sulfur Redox Behavior in Lithium-Sulfur Batteries. *J. Electrochem. Soc.* **2018**, *165* (16), A4027–A4033.
(27) Hwang, J.; Kivelson, D.; Plachy, W.; Plachyt, W. ESR Linewidths in Solution. VI. Variation with Pressure and Study of Functional Dependence of Anisotropic Interaction Parameter. *J. Chem. Phys.* **1973**, *58* (4), 1753–1765.
(28) Reichardt, C. Solvatochromic Dyes as Solvent Polarity Indicators. *Chem. Rev.* **1994**, *94* (8), 2319–2358.
(29) Ronald Fawcett, W.; Fedurco, M.; Opallo, M. The Inhibiting Effects of Tetraalkylammonium Cations on Simple Heterogeneous Electron Transfer Reactions In Polar Aprotic Solvents. *J. Phys. Chem.* **1992**, *96* (24), 9959–9964.
(30) Hoon, M.; Fawcett, W. R. Kinetics of the Electroreduction and Electrooxidation of Tetrakis(Dimethylamino)-p-Benzoquinone in Polar Aprotic Solvents. *J. Phys. Chem.* **1997**, *101* (20), 3726–3730.
(31) Winkler, K.; McKnight, N.; Fawcett, W. R. Electron Transfer Kinetics of Tris(1,10-Phenanthroline)Ruthenium(II) Electrooxidation in Aprotic Solvents. *J. Phys. Chem. B* **2000**, *104* (15), 3575–3580.
(32) Miao, W.; Ding, Z.; Bard, A. J. Solution Viscosity Effects on the Heterogeneous Electron Transfer Kinetics of Ferrocenemethanol in Dimethyl Sulfoxide-Water Mixtures. **2002**.
(33) Opałło, M. The Solvent Effect on the Electro-Oxidation of 1,4-Phenylenediamine. The Influence of the Solvent Reorientation Dynamics on the One-Electron Transfer Rate. *J. Chem. Soc. Faraday Trans. 1 Phys. Chem. Condens. Phases* **1986**, *82* (2), 339–347.
(34) Clegg, A. D.; Rees, N. V.; Klymenko, O. V.; Coles, B. A.; Compton, R. G. Marcus Theory of Outer-Sphere Heterogeneous Electron Transfer Reactions: Dependence of the Standard Electrochemical Rate Constant on the Hydrodynamic Radius from High Precision Measurements of the Oxidation of Anthracene and Its Derivatives in

Nonaqueous Solvents Using the High-Speed Channel Electrode. *J. Am. Chem. Soc.* **2004**, *126* (19), 6185–6192.
(35) Abbott, A. P.; Miaw, C. L.; Rusling, J. F. Correlations between Solvent Polarity Scales and Electron Transfer Kinetics and an Application to Micellar Media. *J. Electroanal. Chem.* **1992**, *327* (1–2), 31–46.
(36) Miao, W.; Ding, Z.; Bard, A. J. Solution Viscosity Effects on the Heterogeneous Electron Transfer Kinetics of Ferrocenemethanol in Dimethyl Sulfoxide-Water Mixtures. *J. Phys. Chem. B* **2002**, *106* (6), 1392–1398.
(37) Waldeck, D. H.; Khoshtariya, D. E. Fundamental Studies of Long- and Short-Range Electron Exchange Mechanisms between Electrodes and Proteins. **2011**, 105–238.